International Journal of Parasitology Research
ISSN: 0975-3702&E-ISSN: 0975-9182, Volume 8, Issue 1, 2016, pp.-173-183.
Available online at http://bioinfopublication.org/jouarchive.php?opt=&jouid=BPJ0000241

CLONING AND CHARACTERIZATION OF GENES ENCODING TWO DETOXIFYING ENZYMES, GLUTATHIONE S-TRANSFERASE AND CARBOXYLESTERASE, FROM BURROWING NEMATODE (*RADOPHOLUS SIMILIS*)

ROSANA O.B.[1], EAPEN S.J.[1]*, KRISHNA P.B.[2]
[1]Bioinformatics Centre, ICAR-IISR, Kozhikode, Kerala, India.
[2]Department of Crop Protection, ICAR-IISR, Kozhikode, Kerala, India
*Corresponding Author: Email- sjeapen@spices.res.in , rosana@spices.res.in

Received: October 10, 2015; Revised: January 18, 2016; Accepted: January 19, 2016

Abstract- Background: *Radopholus similis* (Cobb) Thorne is a migratory endoparasitic nematode infesting several tropical and sub-tropical plant species. Computational screening and conserved domain annotation of assembled EST sequences from the burrowing nematode (*R. similis*) revealed seven contigs similar to glutathione S-transferases (GSTs) and four contigs for carboxylesterases / cholinesterases (CESs). One of the contigs corresponding to each gene were cloned from *R. similis* cDNA (KM670018, KP027005) and characterized by phylogeny and structural motif comparison. Glutathione S-transferase is a critical antioxidant and detoxification enzyme and carboxylesterase is responsible for controlling the nerve impulse, detoxification and various developmental functions. Detoxifying ability of these proteins makes them as major targets of pesticides used for plant parasitic nematode (PPN) management.
Methodology: In the present work, both molecular biology and bioinformatics approaches have been used to study two potential target genes of *R. similis*. The study presents 3D-structural models for *Rs*-GST and *Rs*-CES proteins using conventional molecular modeling techniques and structural motifs have been characterized with motif elucidation and sequence analysis methods. Subsequently, consense based phylogenetic analysis approach was followed to define the evolutionary relationships for each target proteins.
Results: We report for the first time the presence and amplification of two novel target genes (GSTs and CESs) from *R. similis*. The structural motif characterization of the two genes with corresponding nematode genes indicated the functional diversity of the conserved motifs present in *Rs*-GST and *Rs*-CES. The search for protein signature motifs through InterProScan analysis confirmed the presence of thioredoxin-like fold (IPR012336), glutathione S-transferase, N-terminal (IPR004045), glutathione S-transferase, C-terminal (IPR010987) and glutathione S-transferase domain (PF00043) for *Rs*-GST and carboxylesterase, type B (IPR002018), alpha/beta hydrolase fold (IPR029058) and carboxylesterase domain (PF00135) for *Rs*-CES. The 3D protein models of each protein were developed through homology modeling and the active-site residues were predicted. Phylogenetic analysis revealed the evolutionary relationships of each target proteins.
Conclusions: Identifying and cloning of genes involved in nematode survival and determining their functions are vital to elucidate the parasitism and host invasion processes of PPNs. The comparative structural analysis and motif characterization of studied targets will probably offer a novel approach for controlling plant nematodes.

Keywords- Burrowing nematode, *Radopholus similis*, plant parasitic nematode, target genes, detoxifying enzymes, glutathione S-transferase, carboxylesterase, motif characterization..

Citation: Rosana OB, et al., (2016) Cloning and Characterization of Genes Encoding Two Detoxifying Enzymes, Glutathione S-transferase and Carboxylesterase, from Burrowing Nematode (*Radopholus similis*). International Journal of Parasitology Research, ISSN: 0975-3702 & E-ISSN: 0975-9182, Volume 8, Issue 1, pp.-173-183.

Introduction

The burrowing nematode *Radopholus similis* (Cobb, 1893) Thorne, 1949 is a migratory endoparasite infesting several tropical and sub-tropical plant species and causing massive plant tissue necrosis because of their active migration through root tissues and destructive feeding on plant cells [1-2]. *R. similis* is known to invade and feed in the cortex of roots of more than 365 plant species [3-6] and is distributed throughout most tropical and subtropical areas, where it severely harms bananas, citrus crops, peppers and many other economically important crops [1-2,7].

Today plant parasitic nematodes (PPNs) are managed with chemical pesticides which are a short-term solution because of the soil inhabitance of nematodes and the perennial nature of crops [8-9]. Presently, the research focus has transferred to molecular biology approaches [10-13] rather than traditional approaches [14-15] for management of nematodes. The esophageal gland secretion proteins [16] and pathogenic genes have been the focus of many studies [10,17-19]. Another target group is antioxidant enzymes that help to defend themselves against reactive oxygen species (ROS) which are produced by the incomplete reduction of oxygen during respiration in mitochondria and as side products of a variety of normal metabolic reactions or from the immune response of the host. Secretory antioxidant proteins produced by PPNs play an important role in diminishing plant defense system and invading host plants [20]. Cloning corresponding genes and determining their functions are important for elucidating the host invasion processes of plant nematodes and will likely provide a new approach to control PPNs [21].

Glutathione S-transferases (GSTs) are widely distributed among all living cells and are a major cellular detoxification system via catalyzing toxin conjugation with reduced glutathione (GSH) or passively binding to various exogenous /endogenous toxic molecules. They comprise a large family of multifunctional dimeric enzymes that are encoded by multigene families involved in the metabolization of a broad variety of xenobiotics and reactive endogenous compounds. GSTs have been exploited as potential target for many chemotherapeutic agents [22-26]. Detoxifying enzyme, GSTs belongs to a protein family involved in critical antioxidant and detoxification of xenobiotics, protection from oxidative damage and intracellular transport of hormones, endogenous metabolites and exogenous chemicals [27-28]. Functions of GSTs have been investigated in helminth parasites, not least because they have been identified as potential vaccine candidates in digeneans [29].

Carboxylesterases (CESs) is a cytoplasmic enzyme which plays a critical role in

neutralizing xenobiotics and plays an important role in the metabolism of organophosphates [30-31]. Carboxylesterases detoxify organophosphate (OP) and carbamates (CB) pesticides and synthetic pyrethroid (SPs) by two main ways, hydrolysis of the ester bond and binding of the pesticide (OP) to the active site of CESs [32].

OP and CB pesticides obtain toxicity from their ability to inhibit many metabolic and physiological enzymes like acetylcholinesterase (AchE), cytochrome P450, protein kinase C, CESs and GSTs, causing toxicity [33]. Both the enzymes (GSTs and CESs) are potentially involved in the pesticide detoxification [34-35]. Various studies reports that, these enzymes (CESs and GSTs) are commonly used as biomarkers in ecological risk assessment of pesticide contaminated environment [36-38]. Kale and Krishnamoorthy (1982) showed up to 80% inhibition of CESs by carbaryl in the earthworm [39]. Hans *et al.,* (1993) reported the induction of GSTs activity in worms by other pesticides, which showed a maximum induction of 250% by endosulphan [40]. Muthusamy *et al.,* (2011) studied the activity of GSTs and CESs in treated samples at lower and higher pesticide concentration and showed that an increased activity in lower dose for CESs and the activity were decreased in high dose [27]. These studies indicate that xenobiotics can elicit changes in the secretory proteins and this makes both the proteins as major targets for pesticides. Comparative sequences, structural and functional analysis of these enzymes are thus important.

Despite the devastating effects of *R. similis* on crop yields, this nematode is still poorly characterized at the molecular level. This paper reports the cloning and characterization of two genes encoding detoxifying enzymes glutathione S-transferase and carboxylesterase in *R. similis*. The 3-D structural and motif characterization of each protein have been done to understand the detoxification systems. We present structural model for each proteins using conventional molecular modeling techniques. The genetic relationships of each gene between corresponding genes from nematoda, vertebrata and arthropoda have also been examined through phylogenetic analysis.

Materials and methods

Radopholus similis culture and collection

The burrowing nematode, *R. similis* was isolated from black pepper roots and was maintained in carrot disk cultures at ICAR-Indian Institute of Spices Research, Kozhikode. Nematodes aseptically teased out of the carrot disks were rinsed using sterile demineralized water; actively moving nematodes from carrot disk cultures were taken after surface sterilization [41] and transferred to a sterile DEPC treated eppendorf tube.

RNA extraction and cDNA synthesis

Total RNA was extracted from mixed stages of *R. similis* (30,000 nos.) using Qiagen RNeasy Lipid Tissue Mini Kit (QIAGEN GmbH, Germany) according to the manufacturer's instructions. First-strand cDNA synthesize was carried out with 2µg RNA as template extracted using ThermoScientific RevertAid Reverse Transcriptase (Thermo Fisher Scientific Inc., MA USA) in the presence of an oligo (dT) primer (Thermo Fisher Scientific Inc., MA USA). The reaction mixture was taken in sterile, nuclease free tube on ice; the mixture contained 2 µg RNA as template, 0.5 µg oligo $(dT)_{18}$ primer, DEPC-treated water and incubated at 65°C for 5 min and chilled on ice and centrifuged. The mixture was then added to another sterile, nuclease free tube containing 5X reaction buffer, ThermoScientific RiboLock RNase inhibitor (Thermo Fisher Scientific Inc., MA USA), 10 mM dNTP mix and RevertAid reverse transcriptase. The mixture was then mixed gently and incubated for 60 minutes at 42°C and then terminated the reaction by heating at 70°C for 10 minutes. Additionally for the preparation of DNA-free RNA for amplification, removal of genomic DNA from isolated RNA preparation was done using ThermoScientific DNaseI, RNase-free according to manufacturer's protocol.

PCR amplification, cloning and sequencing of genes

Genes of *R. similis* coding for glutathione S-transferase and carboxylesterase were amplified from a mixed stage cDNA pool under standard PCR conditions using corresponding primers designed from assembled *R. similis* EST contigs. The sequences of the primer sets for amplification of *Rs*-GST were forward primer: 5'-CTCATCGCTACATTCATGGTG 3'; reverse primer: 5'- TGTGCTCAGAATTTCTTCATCAG 3'. For amplification of *Rs*-CES, the forward primer:5'- ATGAGCAGATTCACTCGTTCG 3'; reverse primer: 5'-CTGACTGCATCCGGCTATC 3'. PCR amplification reactions were performed in 25 µl reaction mixture containing 1X buffer, 1.5 µM $MgCl_2$ 2, 4 µM dNTPs, 0.5 µM forward and reverse primers, 1 U Taq DNA polymerase, and 1 µl cDNA. The PCR cycling parameters were 94°C initial denaturation for 5 minutes, followed by 35 cycles of amplification, denaturation at 94°C for 1 min; annealing at 60°C (*Rs*-GST) and 62°C (*Rs*-CES) for 1 min; and extension at 72°C for 1 min; and additional polymerization at 72°C for 10 min and hold at 4°C. Amplified fragments were purified from agarose gels using ThermoScientific GeneJET Gel Extraction Kit (Thermo Fisher Scientific Inc., MA USA) and cloned into pGEM-T vector (Promega, Madison USA) with standard protocol. Freshly prepared competent cells of *Escherichia coli* DH5α were transformed with recombinant plasmids and positive clones were selected for plasmid isolation. They were sequenced at Eurofins Genomics India Pvt. Ltd., Bangalore, India and the sequences were then assembled using CAP3 [42].

Sequence analysis and motif characterization

Putative protein sequences were obtained by translating the cDNA sequences using the EMBOSS program TRANSEQ [43]. Protein structure analysis was done with Expasy-Protparam tool [44] to analyze the various physical and chemical parameters of these protein sequences. The computed parameters were theoretical isoelectric point (PI), extinction coefficient, molecular weight, amino acid composition, atomic composition, estimated half-life, instability index, aliphatic index and grand average of hydropathicity (GRAVY). Signal peptides were predicted using SIGNALP 3.0 [45] and SLP-Local (Subcellular Location Predictor based on local features of amino acid sequence) was used to predict the subcellular location proteins [46]. Conserved domains were predicted by NCBI Conserved Domain Database and InterProScan [47]. Sequence alignment of identified *Rs*-GST and *Rs*-CES with corresponding known nematode genes was created with MUSCLE program [48]. Conserved motifs and their relative positions of both the proteins were predicted using MEME Version 4.9.1 [49].

Motif characterization of Rs-GST (KM670018) have been studied using alignment with related glutathione S-transferase protein sequences from other nematodes such as *Caenorhabditis elegans* (NP_506983), *Ancylostoma duodenale* (KIH55339), *Necator americanus* (ACX53261), *Haemonchus contortus* (CDJ94821), *Caenorhabditis brenneri* (EGT52653), *Caenorhabditis remanei* (XP_003109030), *Caenorhabditis briggsae* (XP_002630606) and *Meloidogyne incognita* (ABN64198). Motif characterization of *Rs*-CES (KP027005) have been studied using alignment with related carboxylesterase protein sequences from other nematodes such as *Necator americanus* (ETN81995), *Caenorhabditis elegans* (CAA46899, NP_503411), *Caenorhabditis briggsae* (XP_002647363), *Caenorhabditis remanei* (XP_003110383), *Ascaris suum* (ERG83158, ERG83160), *Strongyloides ratti* (CEF63325).

Evolutionary analysis

A final alignment of 199 amino acids for glutathione S-transferases and 308 for carboxylesterases were used in the analyses. The evolutionary history was inferred using the Bayesian, minimum evolutionary and maximum likelihood analysis. Bayesian analysis was performed in MrBayes version 3.1 [50] with two searches run simultaneously for at least two million generations. Flat Dirichlet priors were used for the gamma shape parameter and the proportion of invariable sites. Three heated chains (temperature 0.2) and one cold chain were used in each search. The parameter was then fixed for a bootstrap analysis with 10,000 replicates. Maximum likelihood and minimum evolutionary analyses were performed using MEGA5 [51]. The analysis involved 25 protein sequences for *Rs*-GST and 23 for *Rs*-CES. Out-group was selected for both the genes as *C. elegans peroxidase gene with accession no. Q95003.1.*

The consensus tree was identified using consense package of Phylip 3.69 [52]. The majority-rule consensus of the bootstrap replicate trees was calculated using consense and seqboot package in the Phylip; which generates a majority rule consensus tree that retains the relationships found in majority of the trees.

Homology modeling and structural analysis

As there were no experimental structures for *Rs*-GST and *Rs*-CES, the 3-D protein structure of *Rs*-GST and *Rs*-CES were generated and model optimization was performed using Modeller 9.10 package [53]. Model assessment was done with PDBsum generate [54] for both *Rs*-GST and *Rs*-CES 3-D protein structures. It includes images of the structure, annotated plots of each protein chain's secondary structure, detailed structural analyses generated by the PROMOTIF program [55], summary PROCHECK results [56]. The protein secondary structure motifs were computed by PROMOTIF and the PROCHECK analyses provide an idea of the stereochemical quality of all protein chains in a given PDB structure using Ramachandran plot [57]. Ramachandran Z-score was determined through Structure validation server of WHAT IF web interface [58]. The modeled structures of *Rs*-GST and *Rs*-CES were compared with other known structures using Dali server [59] to analyze the structural similarities of proteins further.

The template protein for homology modeling was identified using PHYRE2 Protein Fold Recognition Server [60]. The active-sites of each protein were identified using CASTp Server [61] and the 3D molecular structures and active-sites of proteins were visualized with UCSF Chimera [62].

Results

RNA extraction, cloning and amplification

Total RNA isolation could obtain a yield of 644.9 ng/µl total concentration of RNA from *R. similis*. First-strand cDNA was synthesized and species confirmations were done by amplifying cDNA with *R. similis* specific ITS primer. The cloned *Rs*-GST had an amplicon size of 823 bp, while it was 1223 bp in the case of *Rs*-CES. The sequences were submitted in NCBI with accession numbers KM670018, KP027005 for *Rs*-GST and *Rs*-CES, respectively.

Sequence analysis

In-silico BLAST homology searches of the amplified genes from *R. similis* revealed similarity with GSTs and CESs of several other nematodes. *Rs*-GST contains an ORF of 618 bp, coding for a polypeptide of 205 amino acid residues with a predicted molecular mass of 23.702 kDa (residues 1-205) and an isoelectric point of 6.21 [Table-1]. Whereas *Rs*-CES, contains an open reading frame of 852 bp encoding for a precursor protein of 407 amino acid residues with a predicted molecular mass of 58.449 kDa (1-407) and isoelectric point of 4.37. The instability index of proteins was found to be well within the range of less than 40, which indicates both the proteins are stable. *Rs*-GST and *Rs*-CES had GRAVY values less than zero, indicating their hydrophilic nature. The aliphatic index of a globular protein is related to its thermostability and is determined by the volume occupied by the aliphatic amino acids such as leucine, isoleucine, valine and alanine. The aliphatic index values of the given proteins were found to be 68.59 and 78.87, respectively [Table-1]. *In-vivo* half-life is a prediction of the time it takes for half of the amount of protein in a cell to disappear after its synthesis in the cell. The extinction coefficient of the mature glutathione S-transferase protein at 280 nm was 23,170 M^{-1} cm^{-1}. The signaling peptide and targeting peptide prediction (NVISTGRMRR THFACCSTTRISRSRTTATSCLPKDWPES) suggested that the sequenced *Rs*-GST is a mitochondrial protein; and in case of *Rs*-CES, the signal peptide (GEIKHSSELFRAAESGSDILMSQLKMSQLKRAL ITPFGG) suggested that it is located in nucleus or cytosol. The average GC content of all *Rs*-GST was 51.15% and *Rs*-CES was 50.78%.

Table-1 *Protein properties of Rs-GST and Rs-CES*

Target	No. of Amino acids	Molecular Weight (KDa)	Isoelectric Point (pI)	Instability Index	Aliphatic Index	GRAVY	Negative Residues	Positive Residues	Half Life
Rs-GST	205	23.702	6.21	28.11	68.59	-0.405	28	27	>20 hours (yeast, in vivo)
Rs-CES	407	58.449	4.37	32.38	78.87	-0.168	40	50	

BLAST search revealed that the putative sequence shared the highest identity with glutathione S-transferase of *Meloidogyne incognita* (ABN64198) which is a plant-parasitic nematode. The conserved domain search for *Rs*-GST shows similarity to GST_N_Sigma_like (CDD accession No.: cd03039) and GST_C_Sigma_ike (CDD accession No.: cd03192) domains, which indicate *Rs*-GST belonging to class Sigma. The search for protein signature motifs through InterProScan analysis confirmed the presence of glutathione S-transferase, N-terminal (IPR004045), N-terminal thioredoxin-like fold (IPR012336), glutathione S-transferase, C-terminal (IPR010987) and glutathione S-transferase domain (PF00043) for *Rs*-GST.

BLAST search for Rs-CES revealed that the sequence shared highest identity with gut esterase-1 of *Ascaris suum* (ERG83158) which is a parasitic nematode. The conserved domain search for *Rs*-CES shows similarity to carboxylesterase family (pfam00135), esterase_lipase (cd00312) and esterase_lipase superfamily (cl21494), which includes lipases, cholinesterases and carboxylesterases. These enzymes act on carboxylic esters (EC: 3.1.1.1). The catalytic apparatus involves three residues (catalytic triad): a serine, a glutamate or aspartate and a histidine. The search for protein signature motifs through InterProScan analysis confirmed the presence of alpha/beta hydrolase fold (IPR029058), carboxylesterase, type B serine active site/catalytic triad (Ser, Glu and His) (IPR002018), carboxylesterase domain (PF00135), esterase-lipase domain (cl21494) for *Rs*-CES.

Homology modeling and structural analysis

Rs-GST showed highest similarity (40%) with PDB id: 2FNO, which is the X-ray crystal structure of a glutathione s-transferase (atu5508) from *Agrobacterium tumefaciens* at 2.00 a resolution [63]. *Rs*-CES showed highest homology (44%) with 4FG5 [64] which is a crystal structure of alpha-esterase-7 carboxylesterase from *Lucilia cuprina* at 2.19 A° resolutions. Cavity (active-site) prediction was carried out for two proteins. [Fig-1] and [Fig-2] shows the 3D-structure of both the proteins along with active-site (surface representation and residues labelled). The Z-score of the modeled structure of *Rs*-GST, calculated using the Dali server were 44.6 with 2FNO (glutathioneS-transferase from *A. tumefaciens*) [63], and 37.6 with 5GSS (glutathione S-transferase from human) [65]. The Z-score of the modeled structure of *Rs*-CES, calculated using the Dali server was 61.8 with 4FG5 (alpha-esterase-7 carboxylesterase from *Lucilia cuprina*) [64] and 30.8 with 1F8U (human acetylcholinesterase). The Z-score of *Rs*-GST and *Rs*-CES with other proteins in PDB indicated that the structure of modeled proteins is highly similar to known counterparts.

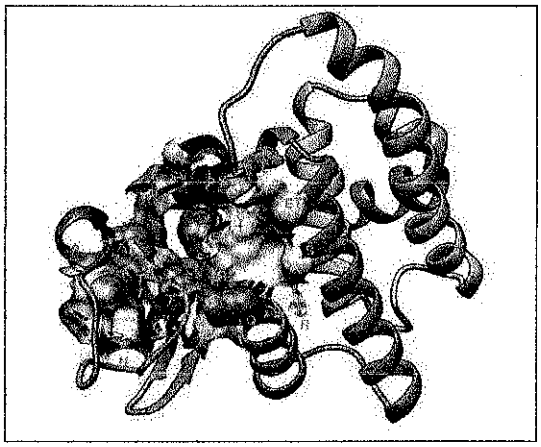

Fig- 1 Shows the 3D-structure of *Rs*-GST along with active-site (surface representation and residues labeled).

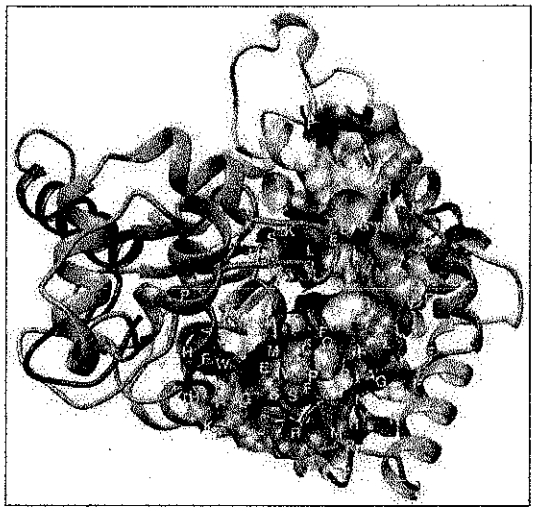

Fig-2 Shows the 3D-structure of *Rs*-CES along with active-site (surface representation and residues labeled).

The secondary structure and Ramachandran plot for *Rs*-GST is displayed in [Fig-3a-3b], which consisted of 10 strands, 123 alpha helices, five helices and the following promotifs: two antiparallel beta sheets, two beta hairpins between strand 1 (Leu52- Ile54) and strand 2 (Glu58- Leu60) and the second between strand 3 (Ile101- Tyr102) and strand 4 (Ala107- Asn108), one antiparallel classic beta bulge, four strands, 13 helices (Thr5-Cys15, Ser17-Ile21, Arg23- Thr26, Cys31-Lys34, Ser63- Phe74, Asp81- Asn100, Pro103- Leu105, Leu109- Val111, Asn118-Gln140, Tyr154- Ser167, Asp172- Glu177, Pro179- Thr190, Ser192- Glu203), 21 helix-helix interactions, eight beta-turns and two inverse gamma turns (Val2- Ser4 and Thr26- Ala28). Ramachandran plot based on an analysis of 118 structures of resolution of at least 2.0 Angstroms and R-factor no greater than 20.0, a good quality model would be expected to have over 90% in the most favored regions [A, B, L]. Ramachandran plot statistics for *Rs*-GST with 204 total residues showed that there were 167 residues (91.3%) in most favored regions [A, B, L]. Additional allowed regions [a, b, l, p] consist of 14 residues (7.7%). There was only one residue falling in generously allowed regions [~a,~b,~l,~p] constituting 0.5%, and one residue in disallowed regions [XX]. There were nine glycine residues and 10 proline residues and 183 non-glycine and non-proline residues.

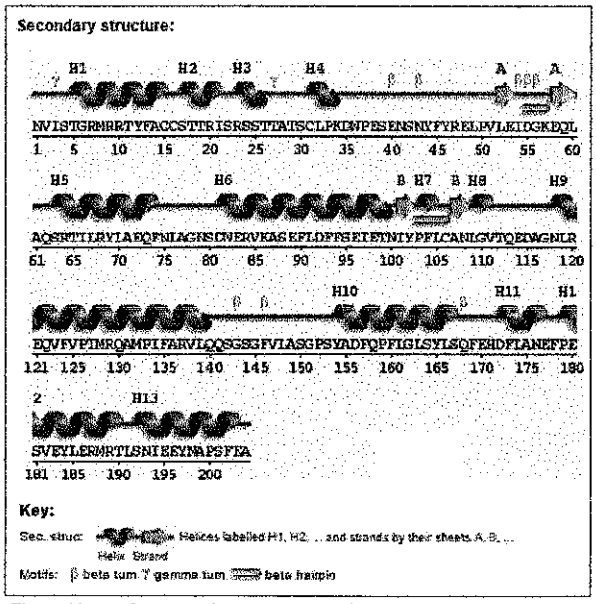

Fig-3a Shows the secondary structure of *Rs*-GST with ten strands, one hundred twenty three alpha helix and five helix

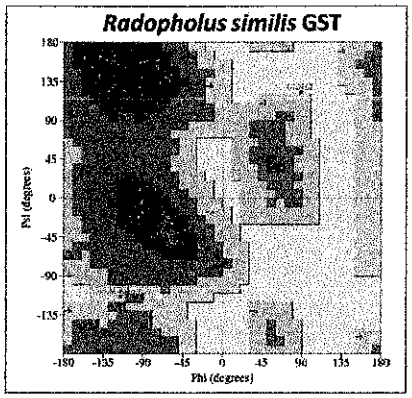

Fig-3b Ramachandran plot for modeled *Rs*-GST showing 91.3% residues in most favored region.

The secondary structure and Ramachandran plot for *Rs*-CES is displayed in [Fig-4a-4b], which consists of 19 strands, 143 alpha helices and 19 helices and the following promotifs: one parallel beta sheet, three beta alpha beta motifs between strand 1 (Thr45- Ile47) and strand 2 (Ser71- Met75), strand 2 (Ser71- Met75) and strand 3 (Val176- Thr181), strand 3 (Val176- Thr181) and strand 4 (Leu292-Met296); four strands as mentioned. Besides, there are 20 helices, 23 helix-helix interactions, 41 beta turns and six gamma turns (Ala13- Ser15, Ile47- Leu49, Ile103-Glu105, Tyr251- Asp253, Ser254- Arg256, and Lys285- Arg287). Ramachandran plot for *Rs*-CES (373 total residues), revealed that there were 287 residues (90.5%) in most favored regions [A, B, L]. In additional allowed regions [a,b,l,p] 25 residues (7.9%) and five 5 residue falling in generously allowed regions [~a,~b,~l,~p] constituting 1.6%, while none in disallowed regions [XX]. There were 30 glycine residues, 24 proline residues and 317 non-glycine and non-proline residues.

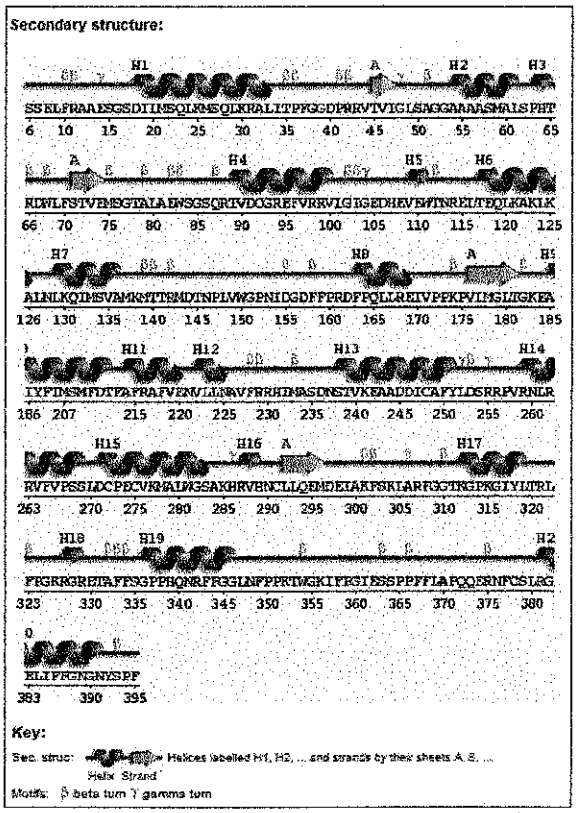

Fig-4a Shows the secondary structure *Rs*-CES with nineteen strand, one hundred forty three alpha helices and nineteen helices

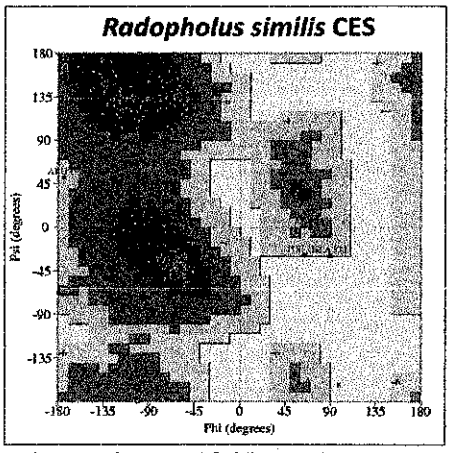

Fig-4b Ramachandran plot for modeled *Rs*-CES showing 90.5% residues in most favored region.

Motif characterization

The comparison of structural features for both the protein sequence revealed that the proteins retained most of the consensus sequence motifs that are crucial in their functions. Distinct motifs were identified to be conserved for both *Rs*-GST and *Rs*-CES.

Comparison of *Rs*-GST (KM670018) with related glutathione S-transferase protein sequences from other nematodes identified conserved motifs for nematode GSTs. Five distinct motifs were identified to be conserved for *Rs*-GST all along the length, which are related to the function and specificity of GSTs. The conserved motifs of *Rs*-GST and their relative positions are displayed in [Fig-5a] and [Fig. 5b]. The InterProScan results showed that the N-terminal domain (G-site) lies between 1-71 bp, so the motif-1, motif-2, motif-3 and motif-4 constitute the G-site and C-terminal domain (H-site) lies between 73-201 bp containing only motif-5. Additionally, the conserved GSH binding site (G-site) (Tyr^{4}, Arg^{16}, Pro^{52}, Asp^{48}, Ser^{56}), and substrate binding pocket (H-site) (Asp^{149}, Pro^{172}) residues in nematode GSTs were identified in the sequence through multiple sequence alignment (MSA) shown in [Fig-6].

The motifs that are conserved among nematode carboxylesterase are identified by aligning *Rs*-CES (KP027005) with related carboxylesterase protein sequences from other nematodes. Four distinct motifs were identified to be conserved for *Rs*-CES all along the length, which are related to the function and specificity of carboxylesterases. The three catalytic residues (catalytic triad): a serine, a glutamate or aspartate and a histidine were contained in the motif regions. The catalytic triad residues (Ser, Asp, His) were contained in Motif 1, motif 3 and motif 4. The conserved motifs of *Rs*-CES and their relative positions are displayed in [Fig-7a] and [Fig-7b]. The three catalytic triad residues of nematode carboxylesterase: a serine, a glutamate or aspartate and a histidine in the motif regions were displayed in multiple sequence alignment [Fig-8]. Mapping conserved motifs of *Rs*-GST and *Rs*-CES onto the 3D structure is displayed in [Fig-9a] and [Fig-9b]; mapping revealed that most of the motif residues were positioned near the catalytic centre of the proteins forming active-sites. Whereas less conserved amino acids occurred more often in the alpha helices of two proteins.

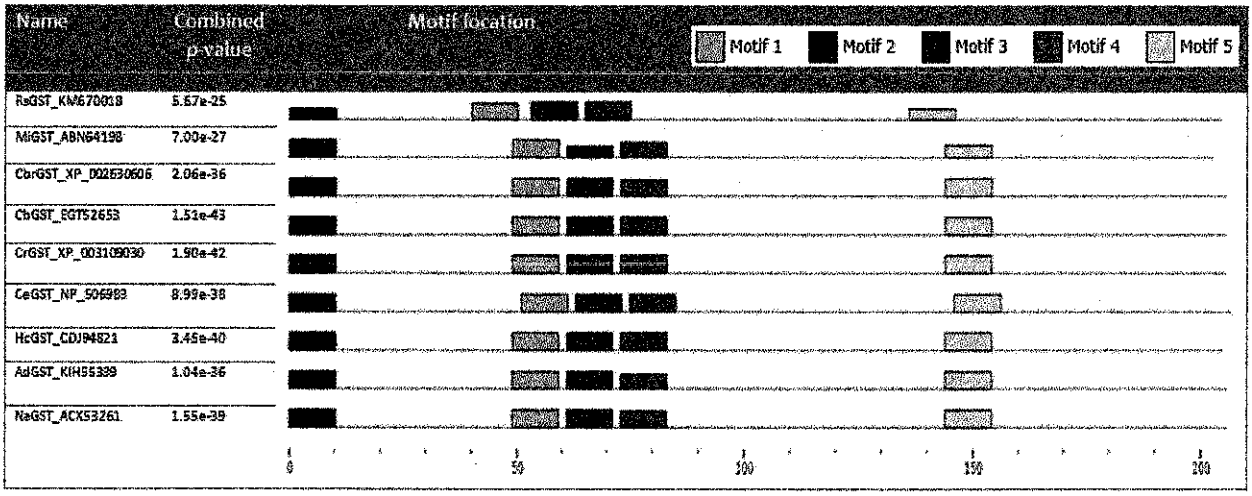

Fig-5a Schematic diagram of conserved amino acid motifs within the nematode GSTs along with *Rs*-GST as analyzed through MEME 4.0 software tool. The black solid line represents different glutathione S-transferase sequences and their length, while colored boxes represent conserved motifs along the length of each sequence.

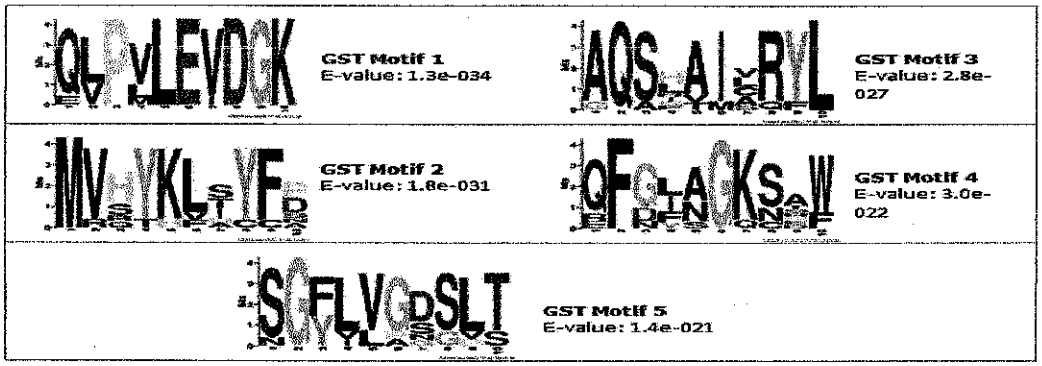

Fig-5b Sequence logo of five prominent conserved motifs in *Rs*-GST and other nematode GSTs.

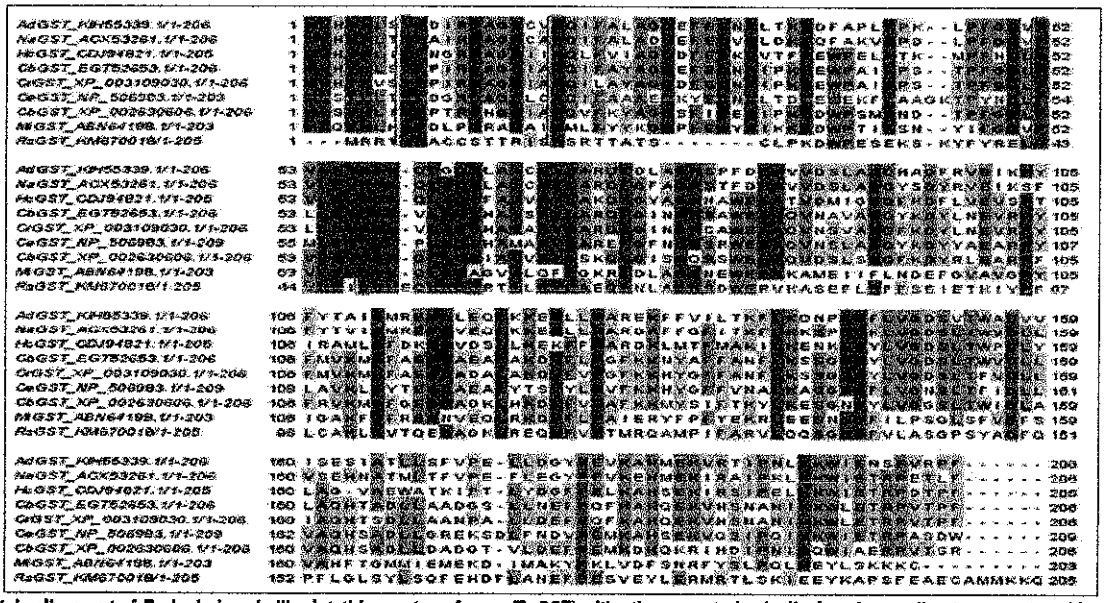

Fig-6 Protein alignment of *Radopholus similis* glutathione-s transferase (RsGST) with other nematodes is displayed according to percentage identity. GSH binding sites (G-sites) (Tyr[4], Arg[16], Pro[52], Asp[48], Ser[55]), are indicated in pink box and substrate binding pocket (H-sites) (Asp[149], Pro[172]) are indicated in yellow box.

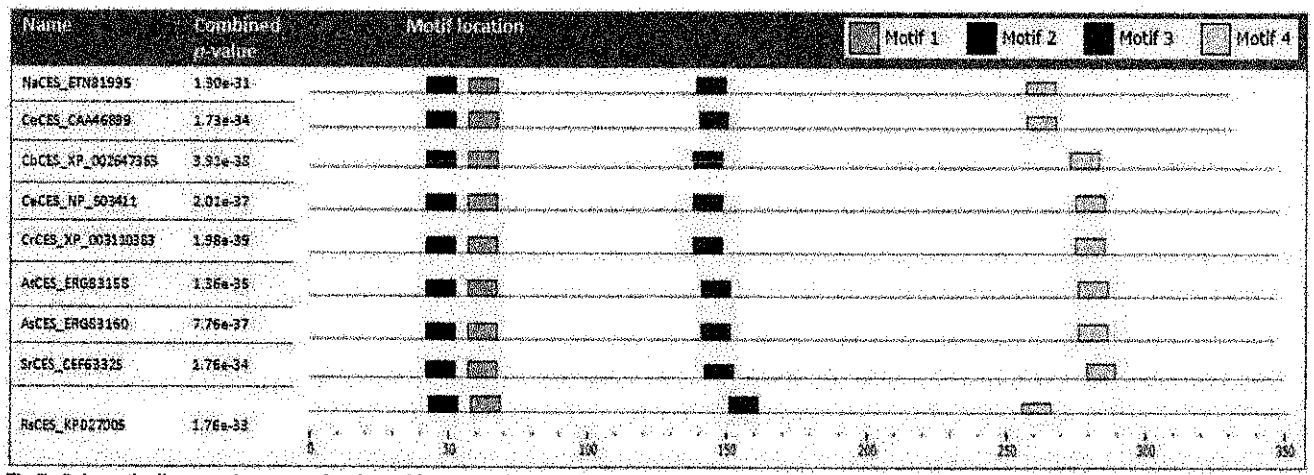

Fig-7a Schematic diagram of conserved amino acid motifs within the nematode carboxylesterase sequences along with *Rs*-CES as analyzed through MEME 4.0 software tool. The black solid line represents different carboxylesterase sequences and their length, while colored boxes represent conserved motifs along the length of each sequence.

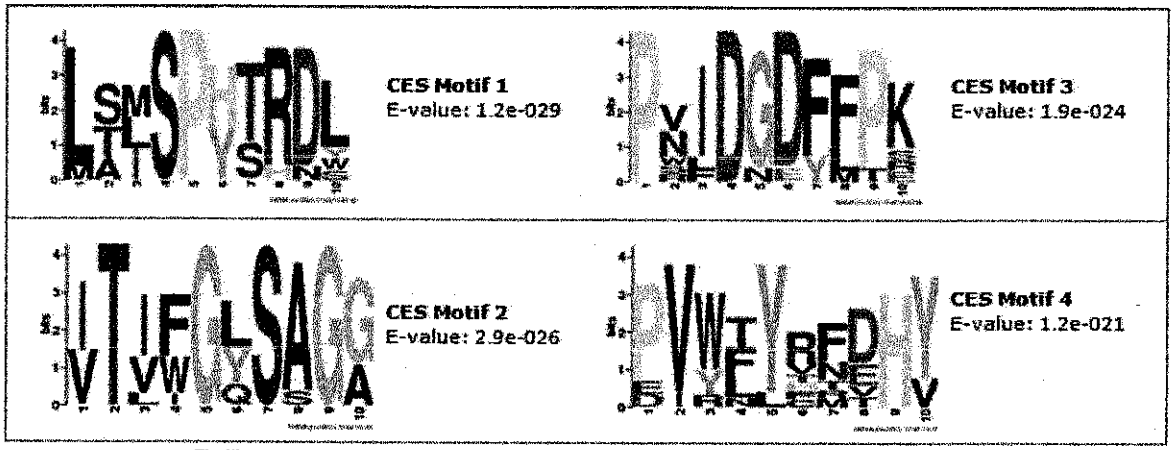

Fig-7b Sequence logo of four prominent conserved motifs in *Rs*-CES and other nematode CESs.

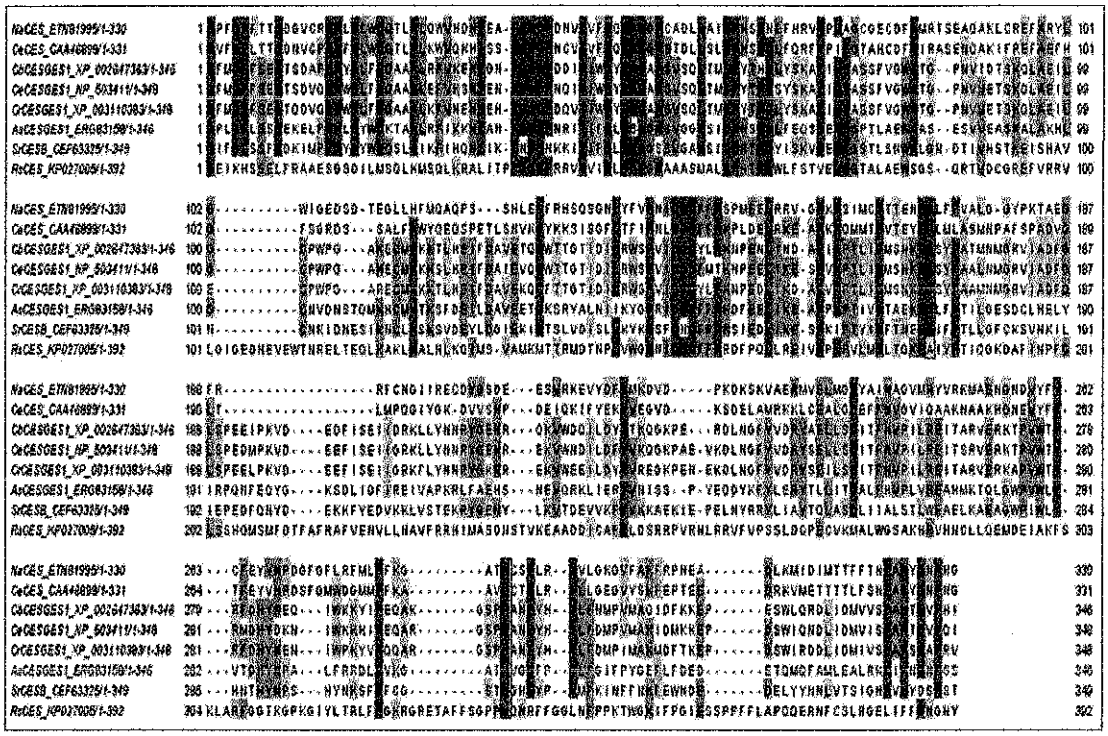

Fig-8 Protein alignment of *Radopholus similis* carboxylesterase (RsCES) with other nematodes is displayed according to percentage identity. The three catalytic residues (catalytic triad): a serine, a glutamate or aspartate and histidine residues were indicated in red color.

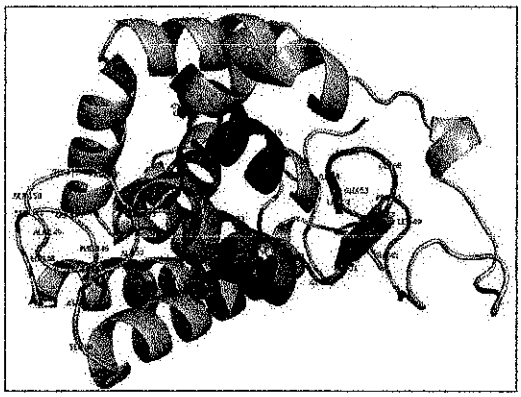

Fig-9a Three-dimensional model of *Rs*-GST, the conserved motifs are indicated in cyans (Motif-1), blue (Motif-2), red (Motif-3), magentas (Motif-4) and Yellow (Motif-5) and non conserved in light blue.

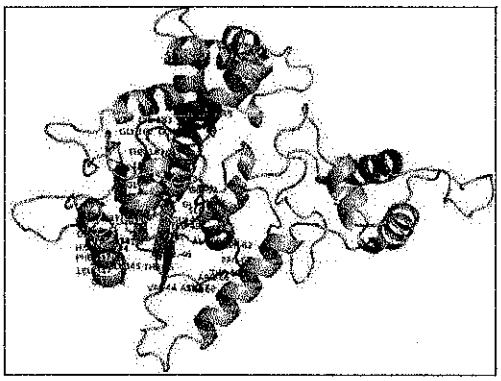

Fig-9b Three-dimensional model of *Rs*-CES, the conserved motifs are indicated in cyans (Motif-1), blue (Motif-2), red (Motif-3), and Yellow (Motif-4) and non conserved in light blue.

Evolutionary analysis

Multiple sequence alignment and motif characterization with other nematodes revealed that the *Rs*-GST and *Rs*-CES retained most of the consensus sequence motifs that are crucial for their function. The phylogenetic results indicated that the GSTs of plant parasites are forming in to a single clade, separated from other nematodes [Fig-10], indicating sequence similarity; *Rs*-GST showed higher similarity to plant-parasitic nematode, *Meloidogyne incognita*, both are grouped together in the phylogenetic tree. Phylogenetic analysis of *Rs*-CES [Fig-11] revealed that it is related to CESs of other nematodes such as *Caenorhabditis elegans*, *C. remanei*, *C. briggsae*, *Strongyloides ratti* and *Ascaris suum*, indicating their sequence similarity. Since carboxylesterase (CES) is sequenced for the first time in *R. similis* and among plant parasitic nematodes, carboxylesterase sequences of other plant parasitic nematodes were not available for the study. *Rs*-CES are closely related to gut esterase 1 (GES) protein of *C. elegans*, *C. remanei*, *C. briggsae*, *S. ratti* and *A. suum*.

Discussion

The migratory plant-parasitic nematode, *R. similis* is a serious problem in many crops and our options to control this nematode are very meager. There is an urgent need to develop novel measures to control them by identifying new molecules and bioagents that act against specific target genes of the nematode. In the present study, an attempt was made to clone and characterize the two detoxification genes *viz.* glutathione S-transferase and carboxylesterase from *R. similis*. Both the genes had signal peptide for secretion and catalytic domains for functional specificity.

The *Rs*-GST had a predicted molecular mass of 23.702 kDa and was well within the range of 21–29 kDa reported for other GSTs [66] and agreed with the previous findings that the average molecular mass of sigma GSTs in parasites is 22 kDa [67]. Further analyses revealed that *Rs*-GST possess all the specific structural features of representatives of GSTs in the Sigma class: a coding domain for the GST_N_Sigma_like (PSSM: cd03039) and another for the GST_C_Sigma_like (PSSM: cd03192). GSTs that share greater than 40% sequence identity are generally included in the same class, and those that possess less than 20–30% sequence identity are assigned to separate classes [68-70]. The signal peptide

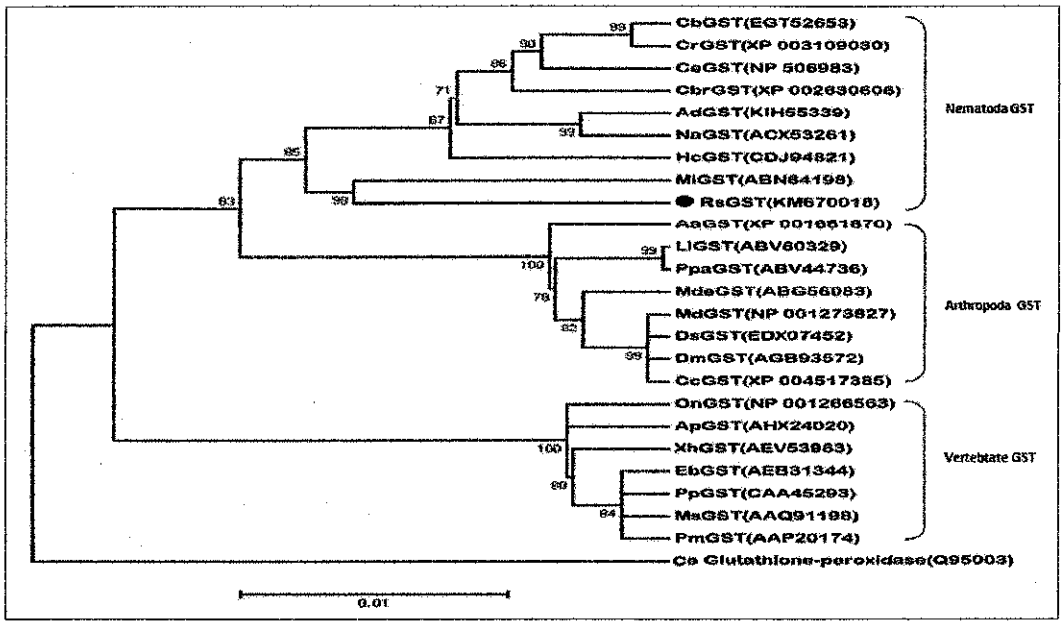

Fig-10 Consensus phylogenetic tree of amino-acid sequence for inferring relationships among GSTs, obtained by Bayesian analysis, Maximum Likelihood and Maximum evolutionary methods. The GenBank accession numbers of each gene are indicated in parentheses. Nodes with better than 60% bootstrap values are indicated with the number of frequency. The *Rs*-GST is indicated by black circle. Ce- *Caenorhabditis elegans*, Ll- *Lutzomyia longipalpis*, Ppa- *Phlebotomus papatasi*, Aa- *Aedes aegypti*, Dm- *Drosophila melanogaster*, Ds- *Drosophila simulans*, Md- *Musca domestica*, Cc- *Ceratitis capitata*, Mde- *Mayetiola destructor*, Ad- *Ancylostoma duodenale*, Na- *Necator americanus*, Hc- *Haemonchus contortus*, Cb- *Caenorhabditis brenneri*, Cr- *Caenorhabditis remanei*, Cbr- *Caenorhabditis briggsae*, Mi- *Meloidogyne incognita*, Rs- *Radopholus similis*, Ms- *Micropterus salmoides*, Pm- *Pagrus major*, Eb- *Epinephelus bruneus*, Pp- *Pleuronectes platessa*, Ap- *Acanthochromis polyacanthus*, On- *Oreochromis niloticus*, Xh- *Xiphophorus hellerii*.

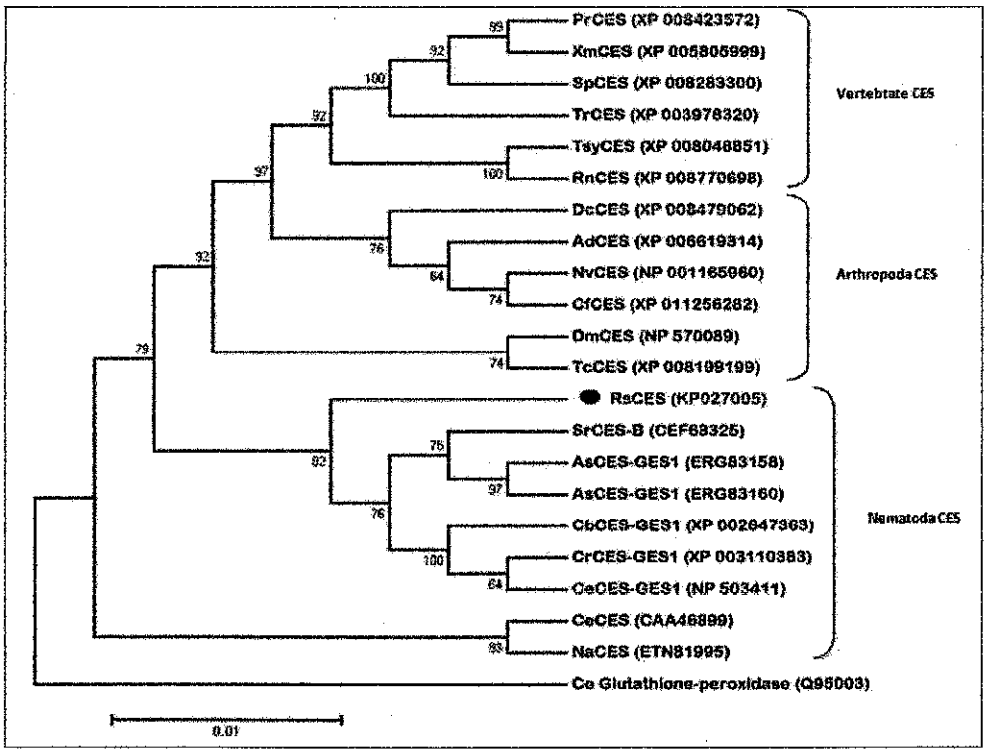

Fig-11 Consensus phylogenetic tree of the amino-acid sequence for inferring relationships among carboxylesterase sequences, obtained by Bayesian analysis, Maximum Likelihood and Maximum evolutionary methods. The GenBank accession numbers of each gene are indicated in parentheses. Nodes with better than 60% bootstrap values are indicated with the number of frequency. The *Rs*-CES is indicated by black circle. Na- *Necator americanus*, Rs- *Radopholus similis*, Ce- *Caenorhabditis elegans*, Cr- *Caenorhabditis remanei*, Cb- *Caenorhabditis briggsae*, Sr- *Strongyloides ratti*, As- *Ascaris suum*, Pr- *Poecilia reticulate*, Xm- *Xiphophorus maculates*, Sp- *Stegastes partitus*, Tsy- *Tarsius syrichta*, Rn- *Rattus norvegicus*, Tr- *Takifugu rubripes*, Nv- *Nasonia vitripennis*, Tc- *Tribolium castaneum*, Ad- *Apis dorsata*, Dc- *Diaphorina citri*, Cf- *Camponotus floridanus*, Dm- *Drosophila melanogaster*.

analysis has indicated *Rs*-GST to be a secretory protein. Therefore, the results suggest that *Rs*-GST characterized here should be a secretory glutathione S-transferase and is affiliated with the Sigma class.

All cytosolic GSTs have the same protein folding, which comprises two domains. The N-terminal domain (domain I) adopts a/b topology and provides the GSH-binding site (G-site). The C-terminal domain (domain II) is an all-a-helical structure and provides the structural element for recognition of a broad range of hydrophobic co-substrates (H-site). The H-site lies adjacent to the G-site and defines the substrate specificity of the enzyme [74-78]. The p-value of the different motifs in *Rs*-GST suggests that glutathione S-transferase motif-1 constituting G-site has diverse amino-acid residues among different nematode species, since it had a higher p-value (1.3e-034) when compared to the other motifs of *Rs*-GST.

The predicted molecular mass of *Rs*-CES, 59.449 kDa and isoelectric point of 4.37 were similar to those of intestinal carboxylesterase of *C. elegans* [71] and *A. suum* [72]. Also, in BLAST search, *Rs*-CES shared highest identity with gut esterase-1 of *Ascaris suum* (ERG83158) which is a parasitic nematode. Further analysis revealed that the *Rs*-CES possess conserved domain specific to carboxylesterase family (pfam00135) such as esterase_lipase (cd00312) and esterase_lipase superfamily (cl21494), which includes lipases, cholinesterases and carboxylesterases. All the three residues specific to catalytic apparatus were well conserved in catalytic triad of *Rs*-CES: a serine, a glutamate or aspartate and a histidine [73]. The presence of signal peptide for *Rs*-CES suggested that the characterized *Rs*-CES is a secretory protein and is affiliated with class of nematode esterase-1.

All the signature motifs of carboxylesterase such as alpha/beta hydrolase fold (IPR029058), carboxylesterase, type B serine active site/catalytic triad (Ser, Glu and His) (IPR002018), carboxylesterase domain (PF00135), esterase-lipase domain (cl21494) were present in characterized *Rs*-CES. The α/β hydrolase fold of carboxylesterase is responsible for the hydrolysis of carboxylesters and amides of various sizes. All carboxylesterase contains an active acylation, site a serine, a glutamate or aspartate and a histidine catalytic triad [79-80]. The p-value of the different motifs in *Rs*-CES suggests that carboxylesterase motif-4 (1.2e-021) constituting a part of catalytic triad is diverse than other motifs.

Rs-GST grouped along with nematode-specific GSTs in phylogenetic analyses and was distinct from those of the vertebrates and insects in the Sigma class GSTs [81-81]. It showed a close relationship with that of *Meloidogyne incognita*. Since both the genes are conserved across different species and genera, in spite of evolutionary pressure for diversification. Consensus based phylogenetic analysis revealed the genetic similarity/diversity of these enzymes with corresponding proteins of other nematodes, arthropoda and vertebrata. However, nematode GSTs are more conserved between the parasitic nematodes (*Ancylostoma duodenale*, *Necator americanus*, *Haemonchus contortus*, *Meloidogyne incognita* and *Radopholus similis*) and diverged from free-living nematodes indicating their possible role for parasitism [Fig-10]. Also phylogenetic analysis suggested that the evolution of nematode GSTs/*Rs*-GST from a common ancestor of Arthropoda GSTs were a relatively recent event. *Rs*-GST together with analyzed nematode GSTs belonged to a clade containing arthropoda GSTs, implying its functional similarity to arthropod GSTs. Whereas *Rs*-CES was closely related to gut esterase 1 (GES) protein of *C. elegans*, *C. remanei*, *C. briggsae*, *S. ratti* and *A. suum* forming a single clade, while normal carboxylesterase of *N. americanus* and *C. elegans* formed an independent clade suggesting their evolutionary distance [Fig-11]. *Rs*-CES was also closely related to CESs of parasitic nematodes. The application of RNAi to the identified detoxification genes in *R. similis* could open the door to unraveling the underlying biology of parasitism in plant parasitic nematodes. The Nematoda CES-GES genes, including *Rs*-CES shared a common ancestor with the arthropoda group including *Tribolium castaneum* and *Drosophila melanogaster*.

Significantly, phylogenetic analysis is in excellent agreement with the multiple sequence alignment result confirming the similarity. The multiple sequence alignment could reveal that, the GSH binding sites (G-sites) (Tyr4, Arg16, Pro52, Asp48, Ser56) and substrate binding pocket (H-sites) (Asp149, Pro172) were conserved in *Rs*-GST [Fig-6], as reported earlier [74-78]. In case of *Rs*-CES, the three catalytic residues (catalytic triad): a serine, a glutamate or aspartate and a histidine residues were highly conserved [Fig-8] among CESs as reported by others [79-80]. The observed results of motif characterization and conservation confirm the phylogenetic relationship of these two genes determined by multiple sequence alignment thus, enhancing the confidence.

In summary, two detoxifying proteins, glutathione s-transferase and carboxylesterase were identified and characterized from *R. similis* that can form the basis towards pathogenicity of plant parasitic nematodes. The results of phylogenetic and motif characterization analysis suggested that the putative proteins encoded by sequenced *Rs*-GST and *Rs*-CES are involved in parasitism of nematode. The identified proteins can act as a valuable resource towards development of target-based nematicides. Along with the information on *C. elegans* glutathione S-transferase and carboxylesterase, the current findings on *Rs*-GST and *Rs*-CES from a burrowing nematode species should provide valuable insights into the evolutionary process and various physiological functions of both the detoxifying genes. The 3D-structures were constructed for both the proteins, as knowledge of the three-dimensional structure is essential for a better understanding of the functional mechanism. After comparative modeling and structural refinement, the general quality of structures was assessed and compared with known structures. We hope that our model will inspire new experimental effort in this area. Furthermore, a better understanding of the 3D-structure and conserved sites comparison of both the enzyme will be pertinent for developing organophosphate based synergists and alternative novel natural nematicides against *R. similis*.

Acknowledgements

We acknowledge with thanks the facilities provided by Director, ICAR- Indian Institute of Spices Research (ICAR-IISR), Kozhikode, Kerala, India; Dept. of Biotechnology (BTISnet), Govt. of India, New Delhi; Distributed Information Sub-Centre (DBT), New Delhi, and the assistance rendered by Mr. OP Nandakishore, PhD Scholar, ICAR-IISR.

References

[1] O'Bannon J.H. (1977) *Journal of Nematology*, 9, 16–25.

[2] Sarah J.L., Pinochet J. and Stanton J. (1996) *The Burrowing Nematode of Bananas, Radopholus similis Cobb, 1913, Musa pest fact sheet, No. 1, International Network for the Improvement of Banana and Plantain*, Montpellier, France.

[3] Brooks F.E. (2008) *Burrowing nematode disease, The Plant Health Instructor*, Doi: 10.1094/PHI-I-2008-1020-01.

[4] Moens M. and Perry R.N. (2009) *Annual Review of Phytopathology*, 47, 313–332.

[5] Rosana O.B., Krishna P.B. and Santhosh J.E. (2014) *International Journal of Computer Applications*, 86, 35–43.

[6] Fogain R. (2000) *Nematology*, 2(2), 129–33.

[7] Luc M., Sikora R. A. and Bridge J. (2005) *Plant Parasitic Nematodes in Subtropical and Tropical Agriculture 2nd Ed. Wallingford, Oxfordshire, UK, CABI Publishing*, pg 616, ISBN 9781845931445.

[8] Siddiqui Z.A. and Mahmoo I., (1999) *Bioresource Technology*, 69, 167–179.

[9] Kerry B.R. (2000) *Annual* Review of *Phytopathology*, 38, 423–441.

[10] Haegeman A., Elsen A., De Waele D. and Gheysen G. (2010) *Molecular Plant Pathology*, 11(3), 315–323.

[11] Zhang C., Xie H., Xu C.L., Cheng X., Li K.M., Li Y. (2012) *European Journal of Plant Pathology*, 133(4), 899–910.

[12] Maier T.R., Hewezi T., Peng J. and Baum T.J. (2012) *Molecular Plant-Microbe Interactions*, 26(1), 31–35.

[13] Zhang C., Xie H., Cheng X., Wang D.W., Li Y., Xu C., Huang X. (2015) *Plos One*, 10 (3), e0118414.

[14] Sarah J.L. (1989) *Nematropica*, 19(2), 199–216.

[15] Dauphin Clermont C., Cabidoche Y.M. and Meynard J.M. (2004) *Soil Use Manage*, 20(2), 105-113.

[16] Smant G., Goverse A., Stokkermans J., DeBoer J.M., Pomp H., Zilverentant J.F., Overmars H.A., Helder J., Schots A. and Bakker J. (1997) *Phytopathology*, 87(8), 839–845.

[17] Jones J.T., Haegeman A., Danchin E.G., Gaur H.S., Helder J., Jones M.G., Kikuchi T., Manzanilla L.R., Palomares-Rius J.E., Wesemael W.M. and Perry R.N. (2013) *Molecular Plant Pathology*, 14(9), 946–961.

[18] Sindhu A.S., Maier T.R., Mitchum M.G., Hussey R.S., Davis E.L., Baum T.J. (2009) *Journal of Experimental Botany*, 60(1), 315–324.

[19] Kimber M.J., McKinney S., McMaster S., Day T.A., Fleming C.C., Maule A.G. (2007) *FASEB Journal.*, 21(4), 1233–1243.

[20] Abad P. and Williamson V.M. (2010) *Advances in Botanical Research*, 53, 147-292.

[21] Davis E.L., Hussey R.S., Baum T.J., Bakker J., Schots A., Rosso M.N., *and* Abad P. (2000) *Annual Review of Phytopathology*, 38, 365–396.

[22] Brophy P.M. and Pritchard D.I. (1992) *Parasitology Today*, 8(12), 419–422.

[23] Brophy P.M. and Barrett J. (1990)*Parasitology* 100 Pt, 2(2), 345-349.

[24] Ahmad R. Srivastava A.K. (2007) *Parasitology* Research, 100, 581–588.

[25] Ahmad R. Srivastava A.K. (2008)*Parasitology Research*, 102, 805–807.

[26] Bhargavi R., Vishwakarma S. and Murty U.S. (2005)*Bioinformation* 1(1), 25-27.

[27] Muthusamy, Shivakumar, Karthi, Ramkumar (2011)*Egyptian Academic Journal of Biological Sciences*, 3 (1), 51- 57.

[28] Clark A., Shamaan N., Sinclair M. and Deuterman W. (1986) *Pesticide Biochemistry and Physiology*, 25(2), 169- 175.

[29] Brophy P.M. and Pritchard D.I. (1994) *Experimental Parasitology*, 79(1), 89-96.

[30] Tang Z.H. and Zhou C.L. (1993) *Acta Entomologica Sinica*, 36(001), 8–13.

[31] Tang Z. H.; Wood R. J.; and Cammak S. L. (1990) *Pesticide Biochemistry and Physiology*, 37, 192-199.

[32] Crow J. A., Potter P. M., Borazjani A., and Ross M. K. (2007) *Toxicology & Applied Pharmacology*, 221(1), 1-12.

[33] Fukuto T.R. (1990) *Environmental Health Perspectives*, 87, 245-54.

[34] Johnson G. and Moore S.W. (2012) *Comparative Biochemistry and Physiology*, 7D, 83–93.

[35] Dixon D.P., Skipsey M. and Edwards R. (2010) *Phytochemistry*, 71(4), 338–350.

[36] Wheelock C.E., Phillips B.M., Anderson B.S., Miller J.L., Miller M.J. and Hammock B.D. (2008) *Reviews of Environmental Contamination and Toxicology*, 195, 117-78.

[37] Olawale Otitoju, Ikechukwu N. E. Onwurah (2007) *African Journal of Biotechnology*, 6, 1455-1459.

[38] Velki M. and Branimir K. Hackenberger (2013) *Chemosphere*, 90, 1216–1226.

[39] Kale R.D. and Krishnamoorthy R.V. (1982)*Current Science*, 51(18), 885-886.

[40] Hans R.K., Khan M.A., Farooq M. and Beg M.U. (1993) *Soil Biology and Biochemistry*, 25(4), 509-511.

[41] O'Bannon J.H. and Taylor A.L. (1968) *Phytopathology*, 58, 385.

[42] Huang X. and Madan A. (1999) *Genome Research*, 9, 868-877.

[43] Rice P., Longden I., Bleasby A. (2000) *Trends in Genetics*, 16, 276-7.

[44] Gasteiger E., Hoogland C., Gattiker A., Duvaud S., Wilkins M.R., Appel R.D. and Bairoch A., (In) John M. Walker (ed), (2005) *The Proteomics Protocols Handbook*, Humana Press, 571-607.

[45] Bendtsen J.D., Nielsen H., von Heijne G. and Brunak S. (2004) *Journal of Molecular Biology*, 16, 340(4), 783-95.

[46] Matsuda S., Vert J.P., Saigo H., Ueda N., Toh H., Akutsu T. (2005) *Protein Science*, 14(11), 2804-2813.

[47] Quevillon E., Silventoinen V., Pillai S., Harte N., Mulder N., Apweiler R., and Lopez R. (2005)*Nucleic Acids Research*, W116–W120.

[48] Edgar R.C. (2004) *Nucleic Acids Research*, 32(5), 1792-1797.

[49] Timothy L. Bailey, Mikael Bodén, Fabian A. Buske, Martin Frith, Charles E. Grant, Luca Clementi, Jingyuan Ren, Wilfred W. Li and William S. Noble (2009)*Nucleic Acids Research*, 37, W202-W208.

[50] Ronquist F., Huelsenbeck J.P. (2003) *Bioinformatics* 19, 1572–1574.

[51] Tamura K., Dudley J., Nei M., and Kumar S. (2007) *Molecular Biology and Evolution*, 24, 1596-1599.

[52] Felsenstein J. (1981) *Journal of Molecular Evolution*, 17 (6), 368–376.

[53] Eswar N., Marti-Renom M. A., Webb B., Madhusudhan M. S., Eramian D., Shen M., Pieper U. and Sali A. (2006) Comparative Protein Structure Modeling With MODELLER, *Current Protocols in Bioinformatics, John Wiley & Sons, Inc., Supplement* 15, 5.6.1-5.6.30.

[54] Laskowski R. A. (2001) *Nucleic Acids Research*, 29(1), 221-222.

[55] Hutchinson E.G. and Thornton J.M. (1996) *Protein Science*, 5(2), 212-220.

[56] Laskowski R.A., MacArthur M.W., Moss D.S. and Thornton J.M. (1993) *Journal of Applied Crystallography*, 26, 283-291.

[57] Rob W.W. Hooft, Chris Sander and Gerrit Vriend (1997) *Computer Applications in the Biosciences*, 13 (4), 425-430.

[58] Vriend G., (1990) *Journal of Molecular Graphics*, 8, 52-56.

[59] Holm L. and Rosenstrom P. (2010) *Nucleic Acids Research*, 38, W545-549.

[60] Kelley L.A. and Sternberg M.J.E. (2009) *Nature Protocols* 4(3), 363–371.

[61] Liang Jie, Edelsbrunner Herbert and Woodward Clare (1998) *Protein Sciene*, 7, 1884-1897.

[62] Huang C.C., Couch G.S., Pettersen E.F., and Ferrin T.E. (1996) *Pacific Symposium on Biocomputing*, 1, 724.

[63] Kosloff M., Han G.W., Krishna S.S., Schwarzenbacher R., Fasnacht M., Elsliger M.A., Abdubek P., Agarwalla S., Ambing E., Astakhova T., Axelrod H.L., Canaves J.M., Carlton D., Chiu H.J., Clayton T., DiDonato M., Duan L., Feuerhelm J., Grittini C., Grzechnik S.K., Hale J., Hampton E., Haugen J., Jaroszewski L., Jin K.K., Johnson H., Klock H.E., Knuth M.W., Koesema E., Kreusch A., Kuhn P., O I., McMullan D., Miller M.D., Morse A.T., Moy K., Nigoghossian E., Okach L., Oommachen S., Page R., Paulsen J., Quijano K., Reyes R., Rife C.L., Sims E., Spraggon G., Sridhar V., Stevens R.C., van den Bedem H., Velasquez J., White A., Wolf G., Xu Q., Hodgson K.O., Wooley J., Deacon A.M., Godzik A., Lesley S.A., Wilson I.A. (2006) *Proteins*, 65(3), 527-537.

[64] Jackson C.J., Liu J.W., Carr P.D., Younus F., Coppin C., Meirelles T., Lethier M., Pandey G., Ollis D.L., Russell R.J., Weik M., Oakeshott J.G. (2013) *Proceedings of the National Academy of Sciences* USA 110, 10177-10182.

[65] Oakley A.J., LoBello M., Battistoni A., Ricci G., Rossjohn J., Villar H.O., and Parker M.W. (1997b) *Journal of Molecular Biology* 274, 84-100.

[66] Mannervik B. and Danielson U.H. (1988) *CRC critical* reviews in *biochemistry*, 23, 283–337.

[67] Torres-Rivera A. and Landa A. (2008) *Acta Tropica*, 105(2), 99–112.

[68] Mannervik B. (1996) *Biochemical Society Transactions*, 24, 878–880.

[69] Allocati N., Federici L. and Massulli M., Di Ilio C. (2008) *FEBS Journal* 276, 58–75.

[70] Gupta M.N., Kapoor M., Majumder A. and Singh V. (2011) *Current Science*, 100(8), 1152–1162.

[71] James D. McGhee (1987) *Biochemistry* 26, 4101-4107.

[72] Marie Azzaria, William J. Henzelt and James D. McGhee (1994) *Comparative Biochemistry and Physiology*, 109B, No. 2/3, 225-236.

[73] Masakiyo Hosokawa (2008) *Molecules*, 13, 412-431.

[74] Skopelitou K., Dhavala P., Papageorgiou A.C. and Labrou N.E. (2012) *PLoS ONE* 7(4): e34263.

[75] Honaker M.T., Acchione M., Sumida J.P. and Atkins W.M. (2011) *Journal of Biological Chemistry*, 286(49), 42770–42776.

[76] Axarli I., Dhavala P., Papageorgiou A.C. and Labrou N.E. (2009) *Biochemical Journal*, 422, 247–256.

[77] Norrgard M.A., Hellman U. and Mannervik B. (2011) *Journal of Biological Chemistry*, 286,16871–8.

[78] Federici L., Masulli M., Di Ilio C. and Allocati N. (2010) *Protein Engineering Design and Selection*, 23(9), 743–750.

[79] Sussman J.L., Harel M., Frolow F., Oefner C., Goldman A., Toker L. and Silman I. (1991) *Science*, 253, 872–879.

[80] Cygler M., Schrag J.D., Sussman J.L., Harel M., Silman I., Gentry M.K. and Doctor B.R. (1993) *Protein Science* 2(3), 366-382.

[81] LaCourse E.J., Perally S., Morphew R.M., Moxon J.V., Prescott M., Dowling D.J., Sandra M. O'Neill, Anja Kipar, Udo Hetzel, Elizabeth Hoey, Rafael Zafra, Leandro Buffoni, José Pérez Arévalo and Peter M. Brophy (2012) T *PLOS Neglected Tropical Diseases*, 6(5), e1666.

[82] Xie Y., Zhou X., Chen L., Zhang Z., Wang C., Gu1 X., Wang T., Peng X. and Yang G. (2015) *Baylisascaris schroederi, Parasites & Vectors, 8, 44.*